We are IntechOpen, the world's leading publisher of Open Access books Built by scientists, for scientists

4,800
Open access books available

122,000
International authors and editors

135M
Downloads

Our authors are among the

154
Countries delivered to

TOP 1%
most cited scientists

12.2%
Contributors from top 500 universities

CLARIVATE ANALYTICS BOOK CITATION INDEX INDEXED

WEB OF SCIENCE™

Selection of our books indexed in the Book Citation Index in Web of Science™ Core Collection (BKCI)

Interested in publishing with us?
Contact book.department@intechopen.com

Numbers displayed above are based on latest data collected.
For more information visit www.intechopen.com

11

Broadband and Planar Microstrip-to-waveguide Transitions

Kunio Sakakibara
Nagoya Institute of Technology
Japan

1. Introduction

Millimeter-wave systems consist of various components; MMICs, antennas and other microwave circuits in different transmission lines. Loss at the connections between components is significant problem in the millimeter-wave systems. Transitions between different transmission lines; microstrip line, coplanar line, suspended line, slot line, coaxial cable, waveguide et al. are required in the millimeter-wave band. Accurate impedance matching and complete mode transformation between the different transmission lines are important in the design.

Various kinds of microstrip-to-waveguide transitions have been proposed in the millimeter-wave band. Transitions with short-circuited waveguide of 1/4 guided wavelength on the substrate are very popular (Shin et al., 1988, Leong & Weinreb, 1999) because their principle of mode transformation is simple and almost the same with that of ordinary transitions of a waveguide and a coaxial cable (Collin, 1990). Slot-coupled transitions are also proposed by some authors (Grabherr et al., 1994, Hyvonen & Hujanen, 1996). An additional substrate with a radiating element is needed in the waveguide, although the short-circuited waveguide is not necessary. Single layer microstirp-to-waveguide transitions have been developed in the recent years. The short-circuited waveguide and the additional substrate are not necessary, which is advantageous from the industrial point of view for low cost and high reliability. However, narrow frequency bandwidth is essential disadvantage due to the high-Q resonant structure printed on the substrate (Simon et al., 1998, Iizuka et al., 2002, Sakakibara et al., 2003). Broad frequency bandwidth is obtained by using quasi-yagi antenna printed on the substrate in the waveguide (Kaneda et al., 1999). However, the microstrip line is parallel to the waveguide (Kaneda et al., 1999, Sakakibara et al., 2003), which is a different type from others. Here, we treat the transitions whose microstrip line and waveguide are perpendicular to each other.

We have proposed novel microstrip-to-waveguide transitions based on the ones with short-circuited waveguide, shown in Fig. 1(a), to realize broadband characteristic for uses to the broadband applications and for wide manufacturing-tolerance. No additional parts and no complicated structures are needed to extend the bandwidth. Broad frequency bandwidth is realized only by the change of the printed pattern on the substrate. The short-circuited waveguide is replaced by an additional substrate to compose a planar microstrip-to-

waveguide transition in a multi-layer substrate as shown in Fig. 1(b). Since the short-circuited waveguide of the substrate is filled with dielectric material, the bandwidth is narrower than the transition (a) with the hollow short-circuited waveguide. However, the two substrates are attached accurately and free from fabrication error. A planar transition in a single-layer substrate has been developed (Iizuka et al., 2002). Bandwidth is narrow but the transition consists of only one substrate set on the open-ended waveguide as shown in Fig. 1(c), which is attractive from the industrial point of view. The dependencies to the characteristics of these transitions on geometrical parameters of the structures are examined in detail. Various ways to control bandwidths and center frequencies are presented for required characteristics in the designs of the transitions.

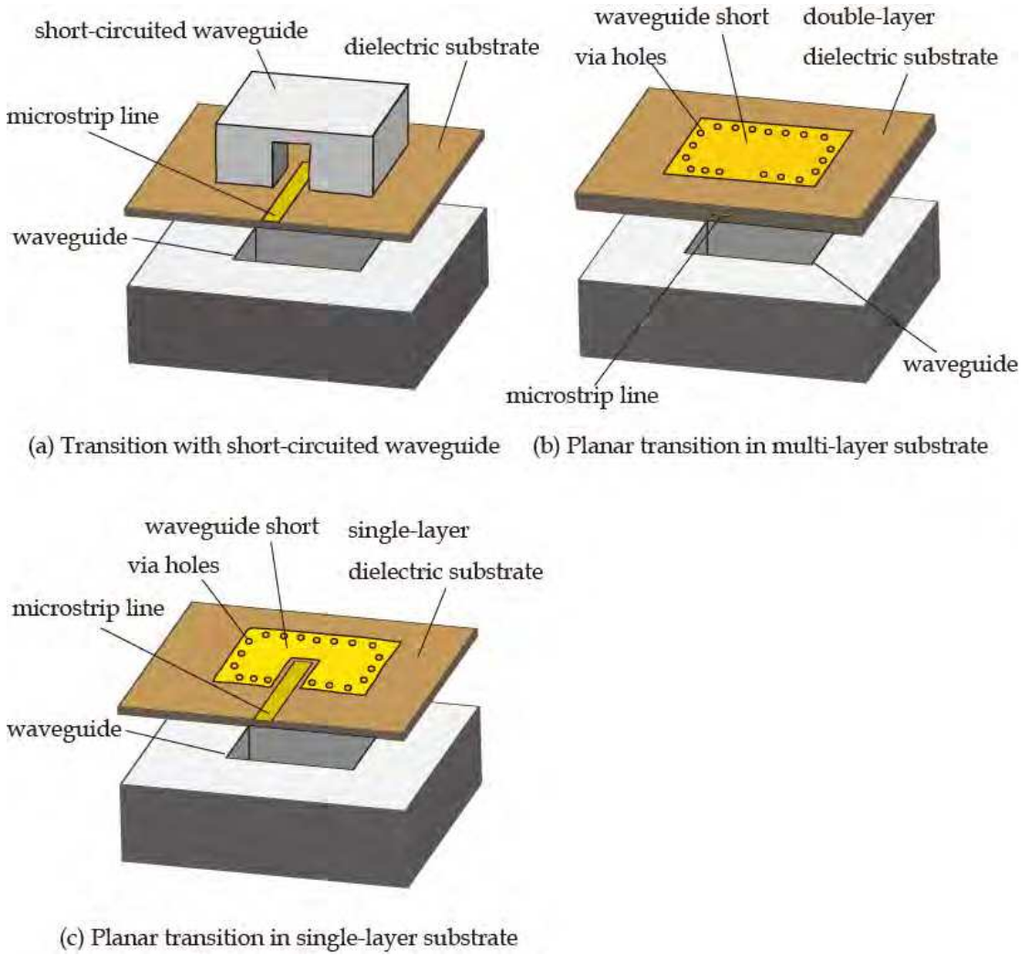

Fig. 1. Variety of microstrip-to-waveguide transitions

2. Configurations of Microstrip-to-waveguide Transitions

Three types of transitions with different features have been developed in the millimeter-wave band. Configurations of the transitions are shown in Fig. 1. The transition (a) with short-circuited waveguide has an advantage of broadband (Deguchi et al., 2005, Deguchi et

al., 2007). However, it requires an additional short-circuited waveguide on the substrate, which suggests the transition suffers from loss increasing due to fabrication error in setting the short-circuited waveguide on the substrate. On the other hand, the planar transition (c) in a single-layer substrate is free from loss increasing due to the fabrication error of the additional parts because the transition consists of only one substrate on the open-ended waveguide (Iizuka et al., 2002). However, bandwidth is narrow since the volume of the resonant circuit is limited in the thin substrate. Planar transition (b) in multi-layer substrate possesses intermediate property between (a) and (c) (Hirono et al., 2007, Sakakibara et al., 2008, Hirono et al., 2008).

2.1 Transition with short-circuited waveguide

Broad operation-bandwidth is in high demand for many applications. Wide tolerance in manufacturing is also advantageous from the industrial point of view. Then, we propose a broadband microstrip-to-waveguide transition with a novel printed pattern in the substrate. No additional parts and no complicated structures are needed. Only the printed pattern is modified in order to extend the frequency bandwidth.

The configuration of the proposed transition is almost the same as more conventional ones that have short-circuited waveguide on the substrate (Shin et al., 1988, Leong & Weinreb, 1999). The microstrip-to-waveguide transition connects a microstrip line and a perpendicular waveguide. A probe at one end of the microstrip line is inserted into the waveguide whose one end is short-circuited. A configuration of the proposed transition is shown in Fig. 1(a). A dielectric substrate with conductor patterns on its both sides is placed on an open-ended waveguide (WR-12, 3.1×1.55 mm). An aperture of the dielectric substrate is covered with an upper waveguide. A short circuit of the upper waveguide is theoretically $\lambda_g/4$ (λ_g : a guided wavelength of the waveguide) above the substrate. Consequently, electric current on the probe couples to magnetic field of TE_{10} dominant mode of the waveguide. Via holes are surrounding the waveguide in the substrate to reduce leakage of parallel plate mode transmitting into the substrate.

Figure 2 shows cross-sectional views of the proposed transition. Two distinctive features are introduced in the upper conductor pattern (AA′ plane) of the dielectric substrate as is shown in Fig. 2(a) and 3. First, the probe is shifted by d toward $+y$-direction from the center of the waveguide ($y = 0$). Local impedance in the waveguide is defined as a ratio of electric field and magnetic field at each point and is lower at $y = d$ rather than at the center of the waveguide where the magnitude of the electric field is the maximum. Therefore, a characteristic impedance of the waveguide becomes comparable with that of the microstrip line (60 Ω, line width: 0.3 mm). Second feature is an extended ground at the opposite side of the waveguide from the probe. The extended ground works as a capacitive obstacle which can control the reactance of the probe (Marcuvitz, 1993). Consequently, impedance matching could be achieved by controlling the shift d of the probe and the length p of the extended ground. The length l of the probe and the length s of the short-circuited waveguide are also important parameters for the performance of the transition. Reducing leakage from the waveguide window at the insertion of the microstrip line, width of the window should be narrower than the width for the cut off condition and is 1.0 mm in this case. Taper structure of 0.5 mm long is adopted for gradually change of impedance. On the other hand in the substrate, cut off condition is much more significant because the wavelength is shorter than

the air. Distance between the via-hole centers is 1.5 mm at the both sides of the probe insertion.

A photograph of the fabricated transition is shown in Fig. 3. Top plate of the short-circuited waveguide is removed to see the inside. Shift d and length l of the probe, length p of the extended ground and length s of the upper waveguide are designed to obtain the required performance. d, l and p are in the printed pattern and s is controlled by the thickness of the metal plate for the short-circuited waveguide shown in Fig. 3.

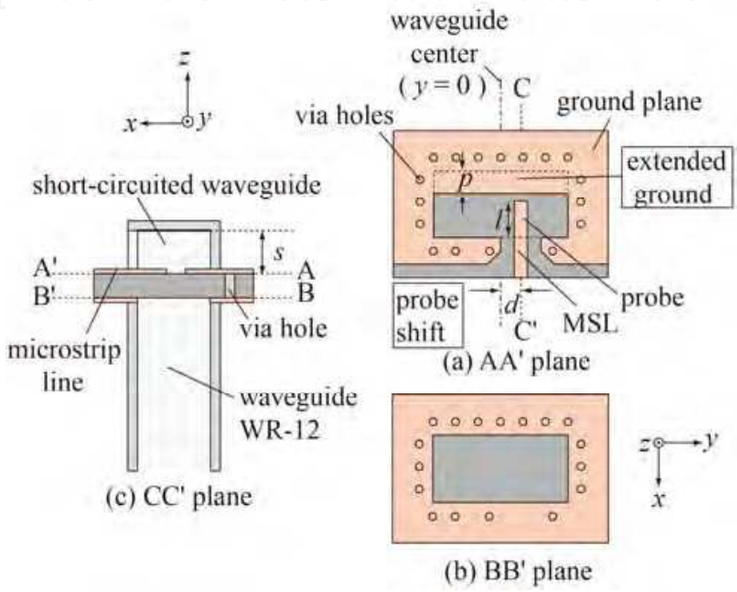

Fig. 2. Structure of the transition with a short-circuited waveguide

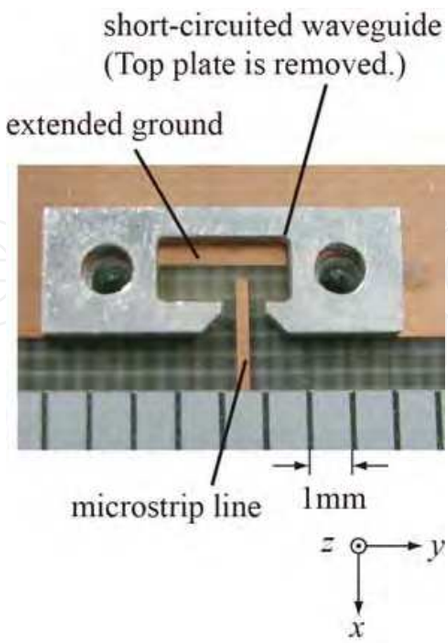

Fig. 3. Photograph of the transition inside

2.2 Planar transition in multi-layer substrate

To reduce the number of required parts and to avoid loss increasing due to alignment error in setting the short-circuited waveguide on the substrate, the short-circuited waveguide is replaced by an additional layer of the substrate, which results in a flat, planar and broadband transition in multi-layer substrate as is shown in Fig. 1(b) and 4. Two layers (Rogers RO4350B, ε_r = 3.48, tanδ = 0.0035) are stuck by an adhesive layer (Rogers RO4450B, ε_r = 3.54, tanδ = 0.004) as shown in Fig. 5. Quasi waveguide is formed in the multi-layer substrate by surrounding via-holes. The top plane is a short circuit of the quasi waveguide. The microstrip line is inserted at the upper plane of the lower substrate into the quasi waveguide with distance of approximately $\lambda_g/4$ away from the short circuit, where λ_g is a guided wavelength in the quasi waveguide. The thickness t_1 of the top layer is optimized as 0.25 mm, while both thicknesses of the lower and the adhesive layers are 0.1 mm.

Metal printed patterns and major parameters are indicated in Fig. 6. Two geometrical features are supplied in the conductor patterns. One is an extended ground as well as the previous transition shown in Fig. 2. Reactance can be controlled by the shunt capacitance caused by the extended ground in the quasi waveguide. Double resonance is expected as the transition with short-circuited waveguide. Probe shift was not applied because it was not necessary for double resonance in this transition. The other feature is the size of the quasi waveguide. The dimensions of the quasi waveguide (2.04 mm X 1.15 mm) composed of via-holes are designed to be smaller than that of the open-ended metal waveguide (WR-10: 2.54 mm X 1.27 mm) in order to suppress the higher order mode in the quasi waveguide because a wavelength in dielectric material is shorter than in the air. Electric field distributions in the transitions with narrow upper waveguide and with wide upper waveguide are shown in Fig. 7 (a) and (b), respectively. The field concentrates around the waveguide center and can couple to the probe in the narrow waveguide (a).

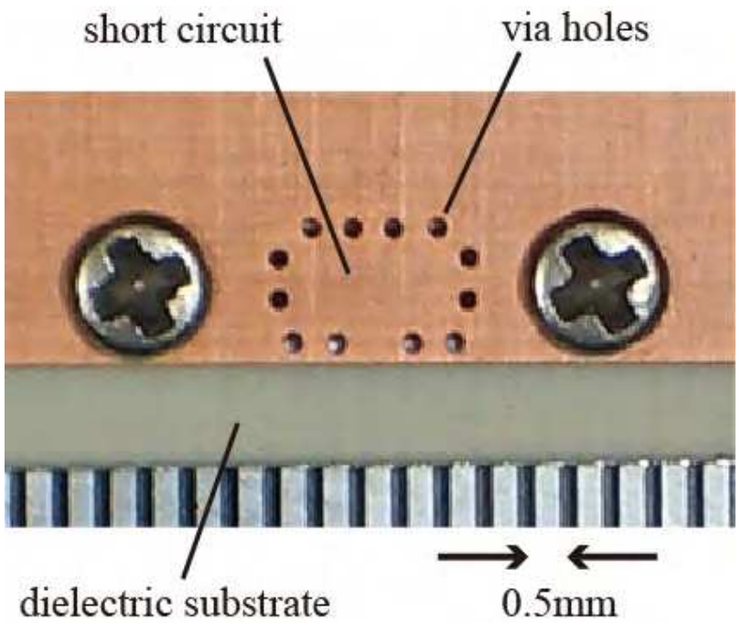

Fig. 4. Photograph of the fabricated planar transition in multi-layer substrate

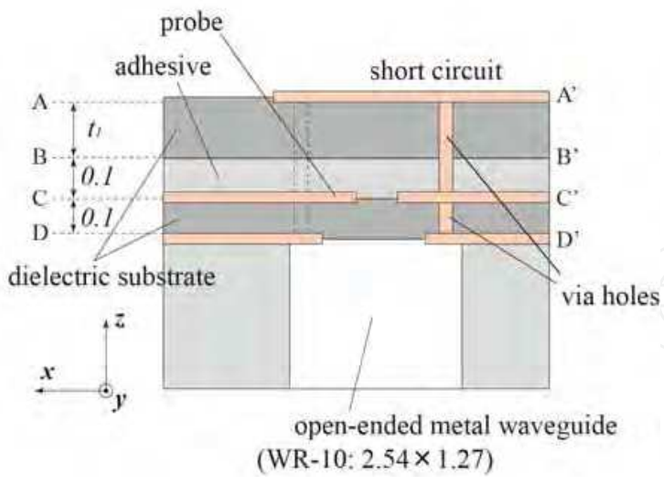

Fig. 5. Cross-sectional view of the planar transition in the multi-layer substrate

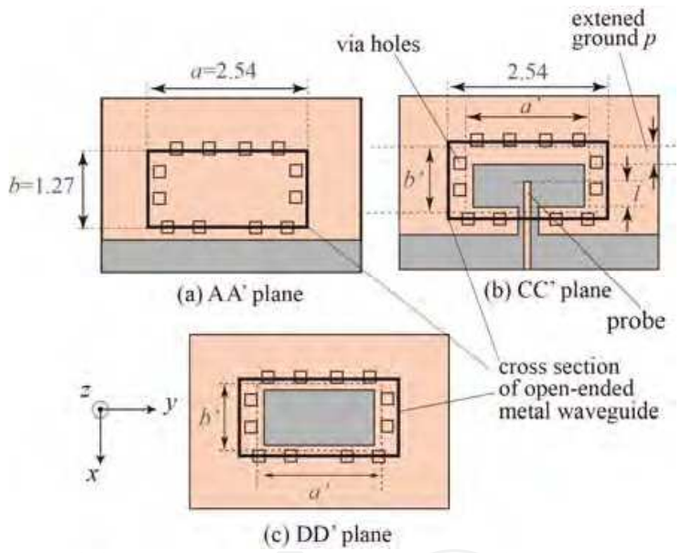

Fig. 6. Printed patterns of the planar transition in the multi-layer substrate

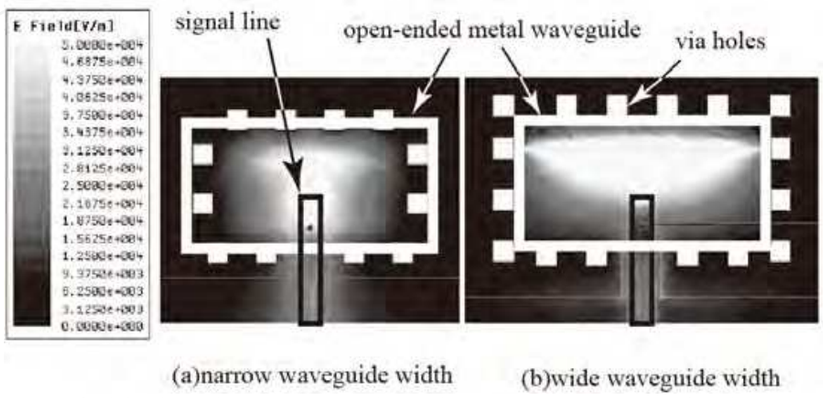

Fig. 7. Electric field distributions in the planar transitions of (a)narrow and (b)wide waveguides

2.3 Planar transition in single-layer substrate

Simple configuration of transition is constructed by setting a single-layer substrate ($\varepsilon_r = 2.2$) on the open ended waveguide (WR-12) as shown in Fig. 1(c). Microstrip line is inserted into the top ground plane to compose partly coplanar line. Via holes surrounds waveguide. The current on the line couples electromagnetically to the current on the patch of the lower plane in the aperture as shown in Fig. 8. Resonant frequency is controlled by the length of the patch and coupling magnitude is controlled by the insertion length of the microstrip line into the ground plane of the waveguide short circuit. Bandwidth would be narrow due to its high-Q characteristic of the patch.

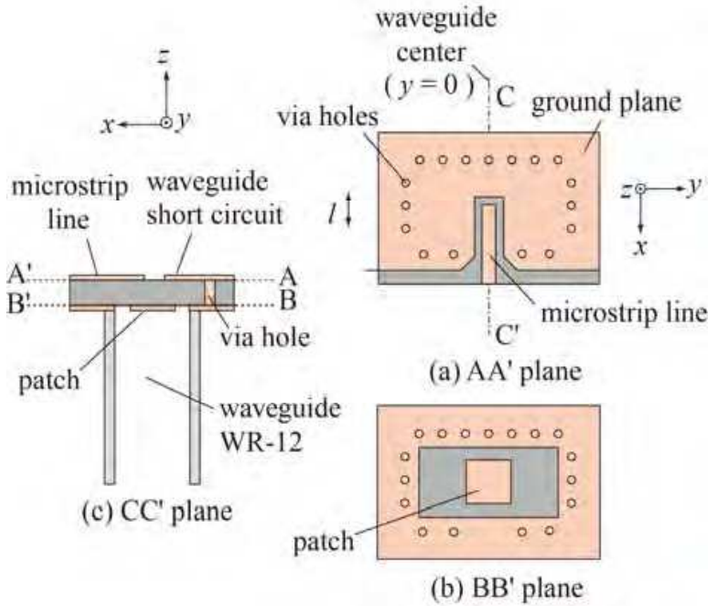

Fig. 8. Cross-sectional view and printed patterns of the transition in the single-layer substrate

3. Performances

3.1 Measurement setup of scattering parameters

Performance of the fabricated transitions is evaluated by experiment in the millimeter-wave band. Scattering parameters are measured in back-to-back configuration as shown in Fig. 9. Microstrip-line ports of two identical transitions are connected by a microstrip line. The other two waveguide-ports of them are connected to the vector network analyzer (Anritsu ME7808B). Frequency dependency of reflection S_{11} for one transition is evaluated by using the time gating function of the vector network analyzer. On the other hand, transmission $S_{21\text{exp}}$ [dB] for one transition is obtained by subtracting the loss of the microstrip line L_{msl} [dB] from the raw data S_{21_raw} [dB] of the two waveguide ports shown in Fig. 9, and dividing by two, that is,

$$S_{21\_\text{exp}} = (S_{21\_\text{raw}}[\text{dB}] - L_{\text{msl}}[\text{dB}]) / 2 \ [\text{dB}] \quad (1)$$

Loss of waveguide is quite small and is neglected in the measurement. Performances of transitions are evaluated by S_{21_exp} in later sections.

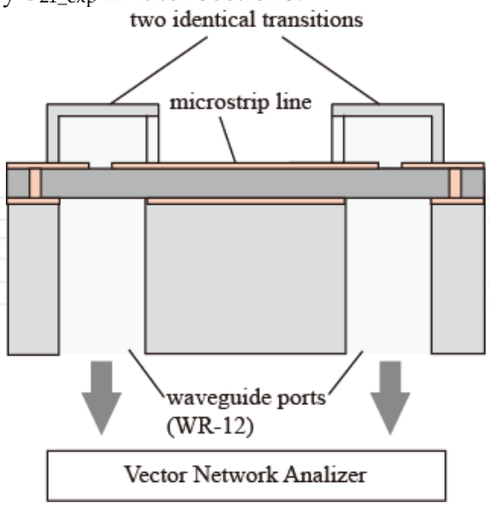

Fig. 9. Measurement setup of the developed transitions

3.2 Transition with short-circuited waveguide

The transitions with short-circuited waveguide are fabricated for experiment as shown in Fig. 3. A Teflon substrate (relative dielectric constant ε_r = 2.2, thickness t = 0.127 mm) with conductor pattern is located on the waveguide aperture. The short-circuited waveguide in the aluminium block is placed on the substrate. All these parts are screwed together. Scattering parameters of reflection S_{11} and transmission S_{21} are calculated by using a commercial electromagnetic simulator of the finite element method. Major parameters indicated in Fig. 2 (the length l and the shift d of the probe, the length p of the extended ground and the length s of the short-circuited waveguide) are optimized so that bandwidth where S_{11} is lower than −30 dB (low-reflection design (1)) or −20 dB (broadband design(2)) becomes the maximum.

Figures 10 and 11 show S_{11} and S_{21} for the transitions of low-reflection design (1) and broadband design (2), respectively. The dimensions are listed in Table 1. The geometrical difference between the designs (1) and (2) is only d. The simulated performance of the conventional transition ($d = p = 0$) is also shown in Fig. 12 for reference. Only l and s are optimized in the condition of no probe shift d = 0 and no extended ground p = 0. Low insertion loss of the proposed ones is achieved such that measured insertion loss is 0.35 dB (design (1)) and 0.33 dB (design (2)) at 76.5 GHz. The simulated loss is almost the same level with the conventional one. Moreover, two resonances are observed in the frequency dependency of S_{11}. Broad frequency bandwidth is obtained such that bandwidth for reflection below −30 dB is 12.9 GHz (16.8 %) in the low-reflection design (1) and that below−20 dB is 24.9 GHz (32.5%) in the broadband design (2). They are 1.95 and 1.37 times as broad as the bandwidth of the conventional ones. The frequency band of S_{11} lower than−20 dB for low-reflection design (1) shifts by only 1 GHz, though both of the two resonant frequencies shift by approximately 3 GHz lower than that of the simulation. Loss increasing due to the frequency shift is quite small because this transition works well over broad frequency bandwidth.

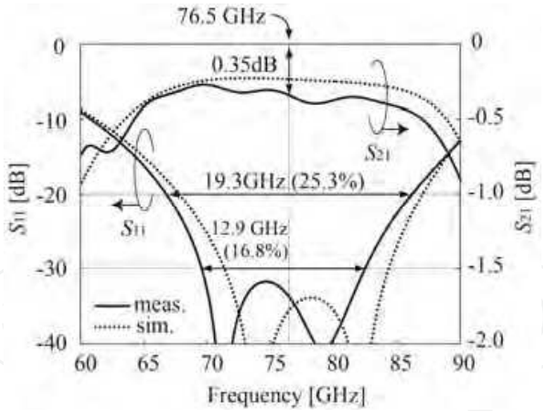

Fig. 10. Meaured and simulated S_{11} and S_{21} of the transition of the low-reflection design (1).

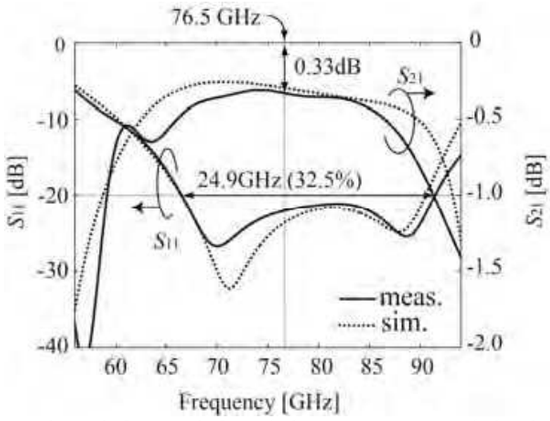

Fig. 11. Measured and simulated S_{11} and S_{21} of the transition of the broadband design (2).

Figures 13 and 14 show measured and simulated S_{11} depending on the shift d of the probe and the length p of the extended ground, respectively. Dependencies on d and p are clarified from the change of the curves. The two resonant frequencies approach as d grows or as p becomes small. Consequently, the number of resonant frequencies becomes one when d is larger than 0.45 mm or p is smaller than 0.50 mm. On the other hand, as d becomes small or as p grows, the interval between the two resonant frequencies extends and the frequency bandwidth becomes broader. Simultaneously, the reflection level at the middle of the two resonant frequencies grows higher. The shift d of the probe and the length p of the extended ground are designed in accordance with the required bandwidth and the admitted reflection level. Measured curves indicated as solid lines almost agree well with the simulated results indicated as dashed line.

Major parameters	Low-reflection design(1)	Broadband design(2)	Conventional design
d [mm]	0.45	0.30	0.00
p [mm]	0.50	0.50	0.00
l [mm]	0.70	0.70	0.72
s [mm]	0.50	0.50	0.71

Table 1. Optimized major parameters

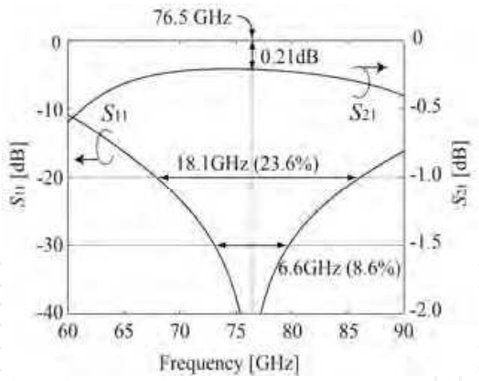

Fig. 12. Measured and simulated S_{11} and S_{21} of the conventional transition

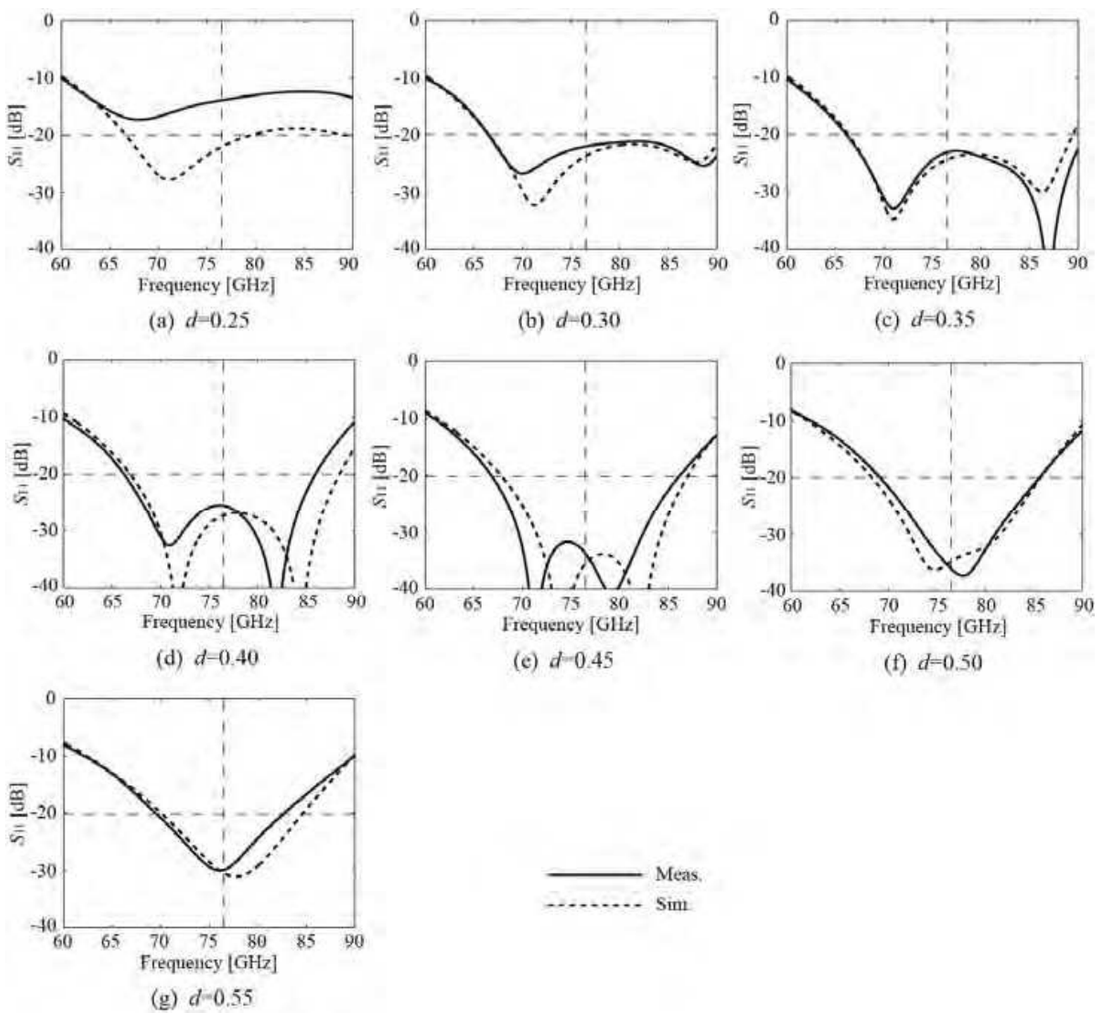

Fig. 13. Measured and Simulated S_{11} variation depending on the parameter d

The change of the resonant frequencies is summarized in Fig. 15. Figure 15(a) shows simulated resonant frequencies versus d when the length p is 0.40, 0.50, and 0.60 mm.

Measured resonant frequency is also shown only for p = 0.50 by dots. No second resonance is observed when p is 0.40 mm even though the shift d of the probe changes from 0.25 up to 0.65 mm. When p is 0.50 mm, only one resonant frequency is observed when d is larger than 0.47 mm. However, two resonant frequencies appear when d is smaller than 0.47 mm. The interval between the two resonant frequencies extends when d becomes small. Next, we investigate the effect of the extended ground as well. Figure 15(b) shows simulated resonant frequencies versus length p of the extended ground when the shift d is 0.30, 0.45, and 0.60 mm. Measured resonant frequency is also shown only for d = 0.45 mm.

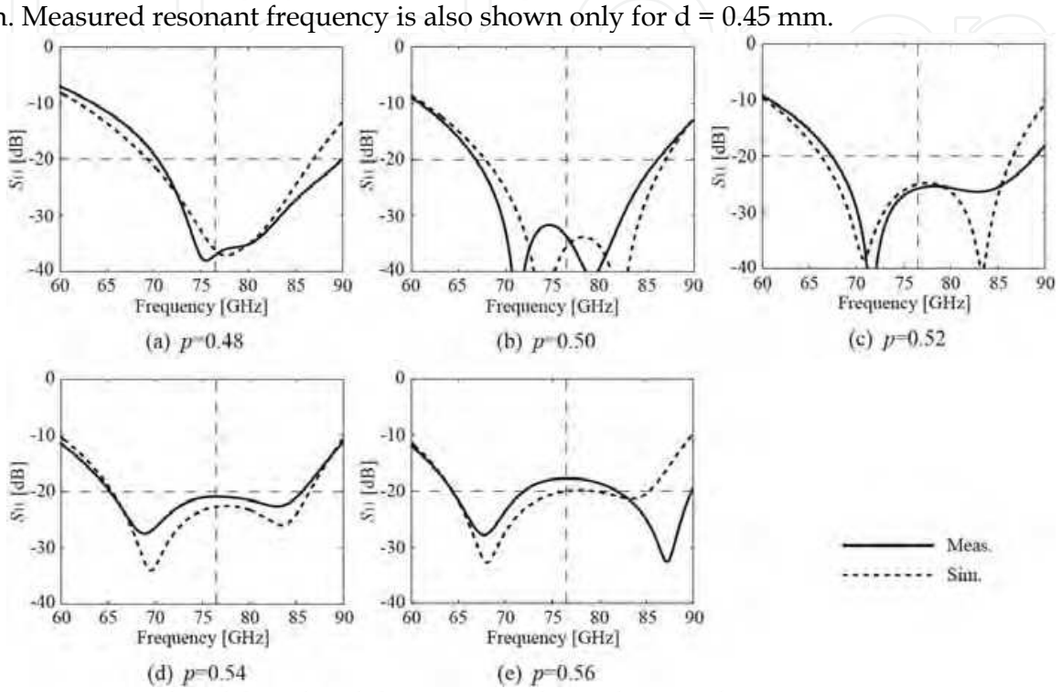

Fig. 14. Measured and Simulated S_{11} variation depending on the parameter p

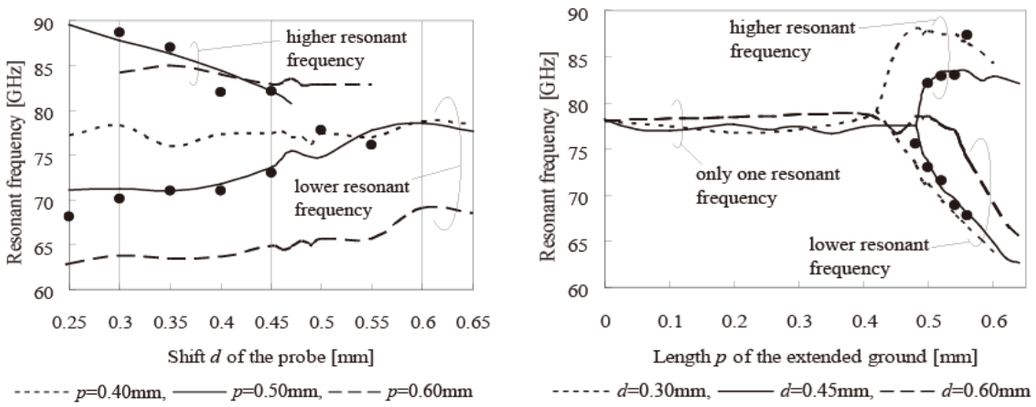

(a) versus shift d of the probe (p = 0.40, 0.50, 0.60 mm)

(b) versus length p of the extended ground (d = 0.30, 0.45, 0.60 mm)

Fig. 15. Simulated resonant frequencies (lines) with measured resonant frequencies (dots)

No second resonance is observed when p is 0.60 mm even though the length p of the extended ground changes from 0.00 up to 0.65 mm. When d is 0.45 mm, only one resonant

frequency is observed when p is smaller than 0.48 mm. However, two resonant frequencies appear when p is larger than 0.48 mm. Furthermore, the higher resonant frequency is almost constant, while the lower resonant frequency shifts low when p becomes large. Consequently, bandwidth can be controlled by changing the two parameters d and p.

3.3 Planar transition in multi-layer substrate

Next, planar transition in multi-layer substrate is designed and its performance is evaluated by simulation and experiments. First, to verify the reason for the double resonance in S_{11}, scattering parameters are investigated by electromagnetic simulation based on the finite element method. Figure 16(a) shows variation of scattering parameters S_{11} and S_{21} depending on the length t_1 of the short-circuited waveguide shown in Fig.5. Lower resonant frequency shifts according to the length t_1 variation, while higher resonant frequency is stable. Consequently, lower resonant frequency is due to the resonance of the short-circuited waveguide. On the other hand, as shown in Fig. 16(b), the higher resonant frequency shifts according to the shift Δx of via-holes located at the opposite side of the microstrip-line probe. Consequently, higher resonant frequency is due to the resonance of the stub composed of the parallel plate waveguide short-circuited by the via-holes. So, the lower and higher resonant frequencies can be independently controlled by the length of the short-circuited waveguide and location of the via holes, respectively.

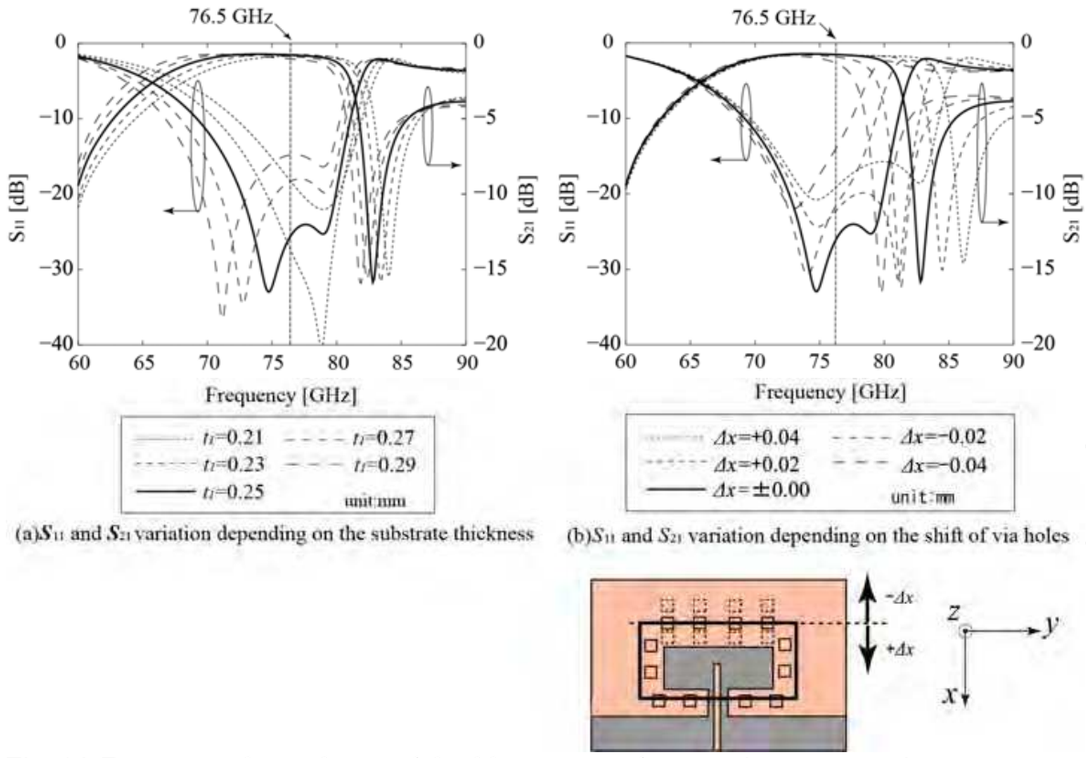

Fig. 16. Parameter dependency of double resonant-frequencies on scattering parameters

The planar transitions in multi-layer substrate are fabricated for experiment as shown in Fig. 4. The multi-layer substrate is fixed on the open-ended waveguide by screws. Surrounding

via holes form the quasi waveguide. The top metal in the via-hole arrangement is short circuit. Scattering parameters of fabricated transitions are measured in the millimeter-wave band. Figure 17 shows the measured S_{11} and S_{21} of the transition. The measured resonant frequencies shift by only 1 GHz lower than the simulated ones. Bandwidth of the transition for reflection lower than –20 dB is 7.0 GHz (9.2 %). Measured insertion loss was approximately 0.7 dB which is the same level with the simulated one.

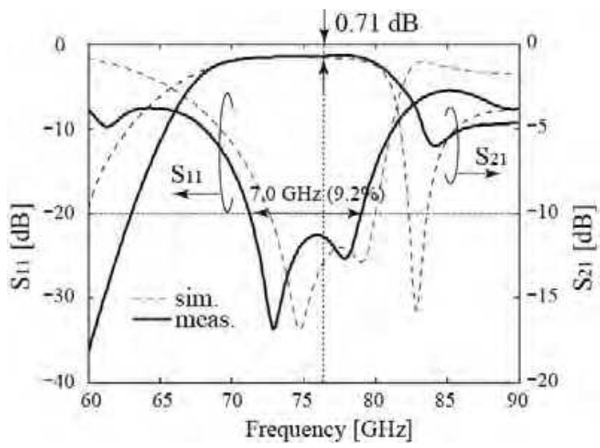

Fig. 17. Measured and simulated S_{11} and S_{21} of the transition in multi-layer substrate

Degradation of matching characteristics due to fabrication error in setting the substrate on the open ended waveguide is examined by electromagnetic simulation. Scattering parameters of the transition with shift of the substrate on the open-ended waveguide in x- and y-directions are shown in Fig. 18. The effect due to the shift of substrate in both x- and y-directions is quite small since the size of the aperture on the lower plane of substrate is much smaller than the waveguide open end and waveguide walls do not affect to the probe current until the waveguide wall appears in the aperture due to the shift. This phenomenon is one of the effective advantages of the transition from the industrial point of view.

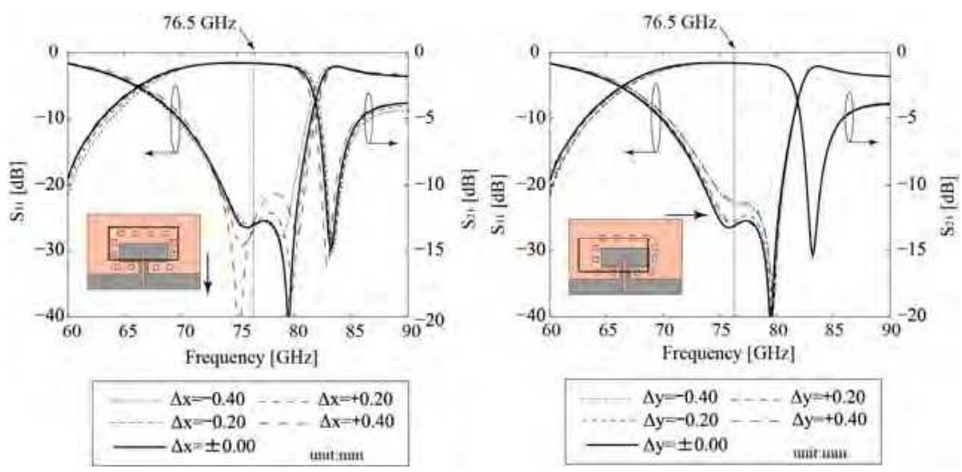

Fig. 18. Scattering parameters of the transition with shift of the substrate on the open ended waveguide in x- and y-directions

3.4 Planar transition in single-layer substrate

The planar transition in single-layer substrate is designed by electromagnetic simulation based on the finite element method. Patch length is designed to obtain resonant frequency at 76.5 GHz. Insertion length of the microstrip line is designed to couple between patch and microstrip line for low reflection-level at the resonant frequency. Figure 19 shows S_{11} and S_{21}. As resonant structure is a patch and is quite smaller size than short-circuited waveguide, Q-factor results high and bandwidth becomes narrow. Thus, bandwidth of reflection lower than –10 dB is approximately 6 GHz.

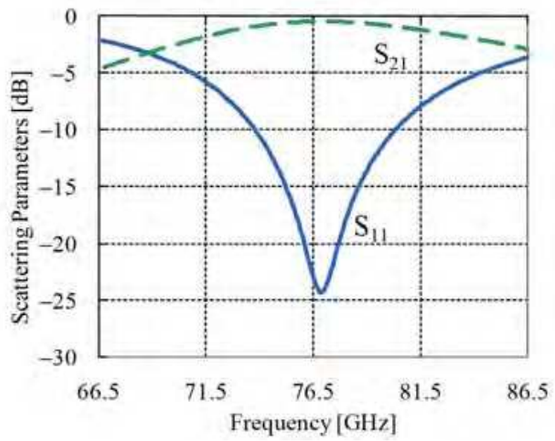

Fig. 19. Scattering parameters of planar transition in single-layer substrate

4. Conclusion

Three types of microstrip-to-waveguide transitions are presented in this chapter. One is a transition with a short-circuited waveguide which is quite broadband such that bandwidth of reflection below −20 dB is 24.9 GHz (32.5 %). However, it requires an additional part of a short-circuited waveguide on the substrate. Second one is a planar transition in multi-layer substrate which is relatively broadband such that bandwidth of reflection below −20 dB is 7.0 GHz (9.2 %) and is composed of the multi-layer substrate. Third one is also a planar transition in single-layer substrate. This is the most cost-effective transition due to its simple structure. However, bandwidth is quite narrow. We can choose the appropriate transition depending on the system requirement.

5. References

Collin, R.E. (1990). *Field Theory of Guided Waves*, Chapter 7, IEEE Press., ISBN: 0-87942-237-8, Piscataway, NJ

Deguchi, Y.; Sakakibara, K.; Kikuma, N. & Hirayama, H. (2005). Millimeter-wave microstrip-to-waveguide transition operating over broad frequency bandwidth, *IEEE MTT-S, Int. Microwave Symp. Dig.*, ISBN: 0-7803-8845-3, Long Beach, CA, June 2005.

Deguchi, Y.; Sakakibara, K.; Kikuma, N. & Hirayama, H. (2007). Design and optimization of Millimeter-wave microstrip-to-waveguide transition operating over broad frequency bandwidth, *IEICE Trans. Electron.*, vol. E90-C, no. 1, Jan. 2007, pp. 157-164, ISSN: 0916-8516

Grabherr, W.; Hudder, B. & Menzel, W. (1994). Microstrip to waveguide transition compatible with mm-wave integrated circuits, *IEEE Trans. Microwave Theory Tech.*, vol.42, no. 9, Sept. 1994, pp.1842-1843, ISSN: 0018-9480

Hirono, M.; Sakakibara, K.; Kikuma, N. & Hirayama, H. (2007). Design of broadband microstrip-to-waveguide transition in multi-layer substrate, Proc. Int. Symp. Antennas and Propag. ISAP2007, 1C5-2, ISBN: 978-4-88552-223-9, pp. 125-128, Sendai, Japan, Aug. 2007

Hirono, M.; Sakakibara, K.; Kikuma, N. & Hirayama, H. (2008). Measured performance of broadband microstrip-to-waveguide transition on multi-layer substrate in the millimeter-wave band, IEICE Trans. Commun., vol. J91-B, no. 9, Sep. 2008, pp. 1057-1065, ISSN: 1344-4697

Hyvonen, L. & Hujanen, A. (1996). A compact MMICcompatible microstrip to waveguide transition, *IEEE MTT-S Int. Microwave Symp. Dig.*, pp.875-878, ISBN: 0-7803-3246-6, San Francisco, CA, June 1996

Iizuka, H.; Watababe, T.; Sato, K. & Nishikawa, K. (2002). Millimeter wave microstrip line to waveguide transition fabricated on a single layer dielectric substrate, *IEICE Trans. Commun.*, vol. E85-B, no. 6, June 2002, pp.1169-1177, ISSN 0916-8516.

Kaneda, N.; Qian, Y. & Ito, T. (1999). A broad-band microstrip-to-waveguide transition using Quasi-Yagi antenna, *IEEE Trans. Microwave Theory Tech.*, vol. 47, no. 12, Dec. 1999, pp.2562-2567, ISSN: 0018-9480

Leong, Y. & Weinreb, S. (1999). Full band waveguide to microstrip probe transition, *IEEE MTT-S Int. Microwave Symp. Dig.*, pp.1435-1438, ISBN: 0-7803-5135-5, Anaheim, CA, May 1999

Marcuvitz, N. (1993). *Waveguide Handbook*, Chapter 5, IEE Press, ISBN: 0-86341-058-8, London, U.K.

Sakakibara, K.; Saito, F.; Yamamoto, Y.; Inagaki, N. & Kikuma, N. (2003). Microstrip line to waveguide transition connecting antenna and backed RF circuits, *IEEE AP-S, Int. Symp. Dig.*, pp.958-961, ISBN: 0-7803-7846-6, , June 2003.

Sakakibara, K.; Hirono, M.; Kikuma, N. & Hirayama, H. (2008). Broadband and Planar Microstrip-to-Waveguide Transitions in Millimeter-Wave Band, Proceedings ICMMT2008, I24A2, pp. 1278-1281, Nanjin, China, April 2008

Shin, Y. C.; Ton, T. N. & Bui, L. Q. (1988). Waveguide-to-microstrip transitions for millimeter-wave applications, *IEEE MTT-S Int. Microwave Symp. Dig.*, pp.473-475, INSPEC Accession Number:3257643, New York, NY, May 1988

Simon, W.; Werthen, M. & Wolff, I. (1998). A novel coplanar transmission line to rectangular waveguide transition, *IEEE MTT-S, Int. Microwave Symp. Dig.*, pp.257-260 ISBN: 0-7803-4471-5, Baltimore, MD, June 1998.

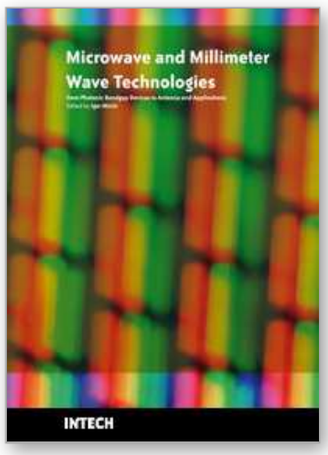

Microwave and Millimeter Wave Technologies from Photonic Bandgap Devices to Antenna and Applications

Edited by Igor Minin

ISBN 978-953-7619-66-4
Hard cover, 468 pages
Publisher InTech
Published online 01, March, 2010
Published in print edition March, 2010

The book deals with modern developments in microwave and millimeter wave technologies, presenting a wide selection of different topics within this interesting area. From a description of the evolution of technological processes for the design of passive functions in milimetre-wave frequency range, to different applications and different materials evaluation, the book offers an extensive view of the current trends in the field. Hopefully the book will attract more interest in microwave and millimeter wave technologies and simulate new ideas on this fascinating subject.

How to reference

In order to correctly reference this scholarly work, feel free to copy and paste the following:

Kunio Sakakibara (2010). Broadband and Planar Microstrip-to-Waveguide Transitions, Microwave and Millimeter Wave Technologies from Photonic Bandgap Devices to Antenna and Applications, Igor Minin (Ed.), ISBN: 978-953-7619-66-4, InTech, Available from: http://www.intechopen.com/books/microwave-and-millimeter-wave-technologies-from-photonic-bandgap-devices-to-antenna-and-applications/broadband-and-planar-microstrip-to-waveguide-transitions

INTECH
open science | open minds

InTech Europe
University Campus STeP Ri
Slavka Krautzeka 83/A
51000 Rijeka, Croatia
Phone: +385 (51) 770 447
Fax: +385 (51) 686 166
www.intechopen.com

InTech China
Unit 405, Office Block, Hotel Equatorial Shanghai
No.65, Yan An Road (West), Shanghai, 200040, China
中国上海市延安西路65号上海国际贵都大饭店办公楼405单元
Phone: +86-21-62489820
Fax: +86-21-62489821

IntechOpen